Natural Product Sciences
21(4) : 240-247 (2015)
http://dx.doi.org/10.20307/nps.2015.21.4.240

Viridicatol from Marine-derived Fungal Strain *Penicillium* sp. SF-5295 Exerts Anti-inflammatory Effects through Inhibiting NF-κB Signaling Pathway on Lipopolysaccharide-induced RAW264.7 and BV2 Cells

Wonmin Ko[1], Jae Hak Sohn[2], Youn-Chul Kim[1,*], and Hyuncheol Oh[1,*]

[1]College of Pharmacy, Wonkwang University, Iksan 570-749, Korea
[2]College of Medical and Life Sciences, Silla University, Busan 617-736, Republic of Korea

Abstract – Viridicatol (**1**) has previously been isolated from the extract of the marine-derived fungus *Penicillium* sp. SF-5295. In the course of further biological evaluation of this quinolone alkaloid, anti-inflammatory effect of **1** in RAW264.7 and BV2 cells stimulated with lipopolysaccharide (LPS) was observed. In this study, our data indicated that **1** suppressed the expression of well-known pro-inflammatory mediators such as inducible nitric oxide synthase (iNOS) and cyclooxygenase (COX)-2, and consequently inhibited the production of iNOS-derived nitric oxide (NO) and COX-2-derived prostaglandin E2 (PGE_2) in LPS stimulated RAW264.7 and BV2 cells. Compound **1** also reduced mRNA expression of pro-inflammatory cytokines such as interleukin-1β (IL-1β), interleukin-6 (IL-6), and tumor necrosis factor-α (TNF-α). In the further evaluation of the mechanisms of these anti-inflammatory effects, **1** was shown to inhibit nuclear factor-kappa B (NF-κB) pathway in LPS-stimulated RAW264.7 and BV2 cells. Compound **1** blocked the phosphorylation and degradation of inhibitor kappa B (IκB)-α in the cytoplasm, and suppressed the translocation of NF-κB p65 and p50 heterodimer in nucleus. In addition, viridicatol (**1**) attenuated the DNA-binding activity of NF-κB in LPS-stimulated RAW264.7 and BV2 cells.
Keywords – Viridicatol, *Penicillium* sp., Marine fungus, Anti-neuroinflammation, Nuclear factor-kappa B (NF-κB)

Introduction

In the course of inflammation, monocytes and macrophages play important roles in mammal cells.[1] One of the immune response to inflammation is triggered by pattern recognition molecule (PAMP), which is recognized by specific receptors such as pattern-recognition receptors (PRR). Upon stimulated with PAMPs in macrophages and microglia, these cells release much of inflammatory mediators, which can be resulted in inflammatory or neuroinflammatory response. Over-activation of these cells leads to the pathogenesis of several neurodegenerative diseases or chronic inflammatory diseases.[2,3] Lipopolysaccharide (LPS), the outer membrane of the gram-negative bacteria, is the most well-known PAMP.[4,5] Recent studies revealed a prominent role in cellular immune responses to LPS, therefore LPS is a useful target for etiological agent of a variety of pathologies. RAW264.7 cells are known as murine macrophages-like cell line, and microglia such as BV2 cells are a type of immortalized murine brain macrophages.[2,3] RAW264.7 and BV2 cells are found to be efficient for testing LPS-induced pro-inflammatory mediators. These cells are widely used to study inflammatory responses characterized by the production of NO, PGE_2, TNF-α, and ILs which can be triggered by LPS.[6,7]

NF-κB is a transcription factor which is implicated in the regulation of many genes that encode mediators of innate immunity and inflammatory responses such as inducible nitric oxide synthase (iNOS) and cyclooxygenase-2 (COX-2).[8] NF-κB is related with an inhibitory protein, inhibitor κB (IκB), which is an inactive form present in the cytoplasm. After activation of NF-κB pathway stimulated by LPS or pro-inflammatory cytokines leads to the phosphorylation of IκB-α kinase (IKK), IκB-α is phosphorylated and degraded inducing translocation of NF-κB into the nucleus.[9] The signaling pathway through NF-κB results in the production of pro-inflammatory cytokines and mediators such as interleukin-1β (IL-1β),

*Author for correspondence
Youn-Chul Kim, College of Pharmacy, Wonkwang University, Iksan 570-749, Republic of Korea
Tel: +82-63-850-6823; E-mail: yckim@wku.ac.kr

Hyuncheol Oh, College of Pharmacy, Wonkwang University, Iksan 570-749, Republic of Korea
Tel: +82-63-850-6815; E-mail: hoh@wku.ac.kr

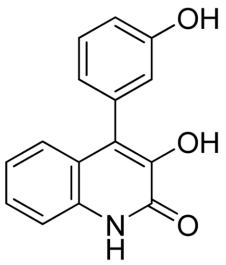

1

Fig. 1. Chemical structure of viridicatol (**1**).

interleukin-6 (IL-6), tumor necrotic factor alpha (TNF-α), iNOS-derived nitric oxide (NO), and COX-2-derived prostaglandin E2 (PGE_2), leading to acute and chronic inflammatory diseases because of cell death against oxidative stress.[10] In the recent studies of molecular target of inflammation, NF-κB has been implicated in the pathogenesis of many inflammation disorders. Numerous plant-derived products have been identified as inhibitors of NF-κB activation and such research has shown the potential agents of anti-inflammatory drugs.[11]

Oceans possess the source of interesting biological and pharmacological properties. Because of the variety of marine species and the diversity of their habitats, some of them have still been less investigated.[12] In this respect, marine environment also provides a lot of unexplored bioactive secondary metabolites from microorganisms. Published papers have shown an enormous increase of microorganisms including marine-derived fungi as potential sources of pharmaceutical leads.[13]

In our previous study, viridicatol (**1**) (Fig. 1) has been isolated from the marine-derived fungal strain *Penicillium* sp. SF5295 as a weak competitive inhibitor of protein tyrosine phosphatase 1B.[14,15] In the course of further biological evaluation of this this quinolone alkaloid, the anti-inflammatory effect of **1** in LPS-stimulated RAW264.7 and BV2 cells was observed, and this study describes the evaluation of anti-inflammatory effects of compound **1** and its possible mechanisms involved in.

Experimental

Materials – Dulbecco's modified Eagle's medium (DMEM), fetal bovine serum (FBS), and other tissue culture reagents were purchased from Gibco BRL Co. (Grand Island, NY, USA). All chemicals were obtained from Sigma Chemical Co. (St. Louis, MO, USA). Primary antibodies, including anti-COX-2, iNOS, IκB-α, p-IκB-α, p50, p65, Actin, PCNA, as well as anti-mouse, goat, and rabbit secondary antibodies were purchased from Santa Cruz Biotechnology (Santa Cruz, CA, USA). Enzyme-linked immunosorbent assay (ELISA) kits for PGE_2, was purchased from R & D Systems, Inc. (Minneapolis, MN, USA). Isolation and structure determination of viridicatol (**1**) has been described elsewhere.[15]

Cell culture and viability assays – RAW264.7 and BV2 cells were maintained at 5×10^5 cells/ml in DMEM medium supplemented with 10% heat-inactivated FBS, penicillin G (100 units/ml), streptomycin (100 mg/ml), and L-glutamine (2 mM), and were incubated at 37 °C in a humidified atmosphere containing 5% CO_2 and 95% air. The effects of the various experimental modulations on cell viability were evaluated by determining the mitochondrial reductase function with an assay based on the reduction of the tetrazolium salt 3-[4,5-dimethylthiazol-2-yl]-2,5-diphenyltetrazolium bromide (MTT) into fomazan crystals.[16] The formation of formazan is proportional to the number of functional mitochondria in the living cells. For the determination of cell viability, 50 mg/ml of MTT was added to 1 ml of cell suspension (1×10^5 cells/ml in 96-well plates) for 4 h. The formazan formed was dissolved in acidic 2-propanol, and the optical density was measured at 540 nm. The optical density of the formazan formed in the control (untreated) cells was considered as 100% viability.

Determination of nitrite (NO production) – The production of nitrite, a stable end product of NO oxidation, was used as a measure of iNOS activity. The nitrite present in the conditioned media was determined by a method based on the Griess reaction.[17] An aliquot of each supernatant (100 μL) was mixed with the same volume of Griess reagent (0.1% (w/v)N-(1-naphathyl)-ethylenediamine and 1% (w/v) sulfanilamide in 5% (v/v) phosphoric acid) for 10 min at room temperature. The absorbance of the final product was measured spectrophotometrically at 540 nm using an ELISA plate reader, and the nitrite concentration in the samples was determined from a standard curve of sodium nitrite prepared in phenol red-free DMEM.

PGE_2 assay – The level of PGE_2 present in each sample was determined using a commercially available kit from R&D Systems (Abingdon, UK). The assay was performed according to the manufacturer's instructions. Briefly, RAW264.7 macrophages and murine peritoneal macrophages were cultured in 24-well plates, pre-incubated for 12 h with different concentrations of compound **1**, and then stimulated for 24 h with LPS. The cell culture supernatants were collected immediately after treatment and centrifuged at $13,000 \times g$ for 2 min to remove the

particulate matter. The medium was added to a 96-well plate pre-coated with affinity-purified polyclonal antibodies specific for PGE_2. An enzyme-linked polyclonal antibody specific for PGE_2 was added to the wells and left to react for 20 h, followed by a final wash to remove any unbound antibody-enzyme reagent. A substrate solution was added, and the intensity of the color produced was measured at 450 nm (correction wavelength set at 540 nm or 570 nm); it was proportional to the amount of PGE_2 present.

Western blot analysis – Western blot analysis was performed by lysing the cells in 20 mM Tris-HCl buffer (pH 7.4) containing a protease inhibitor mixture (0.1 mM PMSF, 5 mg/ml aprotinin, 5 mg/ml pepstatin A, and 1 mg/ml chymostatin). The protein concentration was determined using a Lowry protein assay kit (P5626; Sigma). An equal amount of protein for each sample was resolved by performing 12% sodium dodecyl sulfate-polyacrylamide gel electrophoresis (SDS-PAGE) and then electrophoretically transferred onto a Hybond enhanced chemiluminescence (ECL) nitrocellulose membrane (Bio-Rad, Hercules, CA, USA). The membrane was blocked using 5% skim milk and sequentially incubated with primary antibody (Santa Cruz Biotechnology) and horseradish peroxidase-conjugated secondary antibody, followed by ECL detection (Amersham Pharmacia Biotech, Piscataway, NJ, USA).

Preparation of cytosolic and nuclear fractions – Murine peritoneal macrophages were homogenized (1:20, w:v) in PER-Mammalian Protein Extraction buffer (Pierce Biotechnology, Rockford, IL, USA) containing freshly added protease inhibitor cocktail I (EMD Biosciences, San Diego, CA, USA) and 1 mM phenylmethylsulfonyl fluoride (PMSF). The cytosolic fraction of the cells was prepared by centrifugation at 15,000 × *g* for 10 min at 4 °C. Nuclear and cytoplasmic extracts of murine peritoneal macrophages were prepared using NE-PER nuclear and cytoplasmic extraction reagents (Pierce Biotechnology). After treatment, the murine peritoneal macrophages (3×10^6 cells/3 ml in 60 mm dishes) were collected and washed with phosphate-buffered saline (PBS). After centrifugation, cell lysis was performed at 4 °C by vigorous shaking for 15 min in RIPA buffer (150 mM NaCl, 1% NP-40, 0.5% sodium deoxycholate, 0.1% SDS, 50 mM Tris-HCl [pH 7.4], 50 mM glycerophosphate, 20 mM NaF, 20 mM ethylene glycol tetraacetic acid [EGTA], 1 mM dithiothreitol [DTT], 1 mM Na_3VO_4, and protease inhibitors). After centrifugation at 15,000 × *g* for 15 min, the supernatant was separated and stored at −70 °C until further use. The protein content was determined using the bicinchoninic acid (BCA) protein assay kit.

DNA binding activity of NF-κB – Macrophages were pretreated for 3 h with the indicated concentrations of **1** and stimulated for 1 h with LPS (1 μg/ml). The DNA-binding activity of NF-κB in the nuclear extracts was measured using the TransAM kit (Active Motif, Carlsbad, CA, USA), according to the manufacturer's instructions. Briefly, we added 30 μL complete binding buffer (DTT, herring sperm DNA, and Binding Buffer AM3) to each well. We then added 20 μL of the samples and the indicated concentrations of **1**, and stimulated for 1 h with LPS on macrophages, diluted in complete lysis buffer per well (20 μg of nuclear extract diluted in complete lysis buffer). The plates were incubated for 1 h at room temperature with mild agitation (100 rpm on a rocking platform). After washing each well with wash buffer, 100 μL of diluted NF-κB antibody (1:1000 dilution in 1 × antibody binding buffer) was added to each well, and the plates were incubated for 1 h with mild agitation, as before. After washing each well with wash buffer, 100 μL of diluted horseradish peroxidase (HRP)-conjugated antibody (1:1000 dilution in 1 × antibody binding buffer) was added to each well, and the plates were then incubated for 1 h with mild agitation, as before. Developing solution was added to each well and left to react for 5 min followed by a wash to remove the supernatant. The absorbance was read on a spectrophotometer at 450 nm within 5 min.

Quantitative real-time reverse-transcription polymerase chain reaction – Total RNA was isolated from cells using Trizol from Invitrogen (Carlsbad, CA, USA) following the manufacturer's instructions and quantified spectrophotometrically at 260 nm. Total RNA (1 μg) was reverse transcribed using the High Capacity RNA-to-cDNA kit from Applied Biosystems (Carlsbad, CA, USA). The cDNA was then amplified using the SYBR Premix Ex Taq kit from TaKaRa Bio Inc. (Shiga, Japan) and a StepOnePlus Real-Time PCR system from Applied Biosystems. RT-PCR was performed in a total volume of 20 μL, consisting of 10 μL SYBR Green PCR Master Mix, 0.8 μM of each primer, and diethyl pyrocarbonate-(DEPC-) treated water. The primer sequences were designed using Primer Quest from Integrated DNA Technologies (Cambridge, MA, USA). The primer sequences were as follows: mTNF-α, forward 5'-CCAGACCCTCACACTC ACAA-3', reverse 5'-ACAAGGTACAACCCATCGGC-3', mIL-1β, forward 5'-AATTGGTCATAGCCCGCACT-3', reverse 5'-AAGCAATGTGCTGGTGCTTC-3', mIL-6, forward 5'-ACTTCACAAGTCGGAGGCTT-3', reverse 5'-TGCAAGTGCATCATCGTTGT-3', and mGAPDH, forward 5'-ACTTTGGTATCGTGGAAGGACT-3', reverse 5'-GTAG AGGCAGGGATGATGTTCT-3'. The optimal conditions

for PCR amplification of cDNA were established using the manufacturer's instructions. The mRNA data were analyzed using PCR device of Applied Biosystems (Carlsbad, CA, USA). In addition, the data were analyzed also using StepOne software from Applied Biosystems (Carlsbad, CA, USA), and the cycle number at the linear amplification threshold (Ct) values for the endogenous control mGAPDH and the target gene were recorded. Relative gene expression (target gene expression normalized to the expression of the endogenous control gene) was calculated using the comparative Ct method ($2^{-\Delta\Delta Ct}$).

Statistical analysis – Data are expressed as the mean ± standard deviation (S.D.) of at least 3 independent experiments. To compare 3 or more groups, one-way analysis of variance followed by Tukey's multiple comparison tests was used. Statistical analysis was performed using GraphPad Prism software, version 3.03 (GraphPad Software Inc, San Diego, CA, USA).

Results and Discussion

To exclude the possible cytotoxic effects of compound **1**, the effect of the compound on the viability of RAW264.7 and BV2 cells were determined by MTT assay. As shown in Fig. 2, cell viability of RAW264.7 and BV2 cells was not affected with 5 - 80 μM of **1** for 24 h, however it was decreased at the concentration with 160 μM (Figs. 2A and B). Therefore, in subsequent experiments, the maximum concentration range of **1** was selected by 80 μM in both RAW264.7 and BV2 cells.

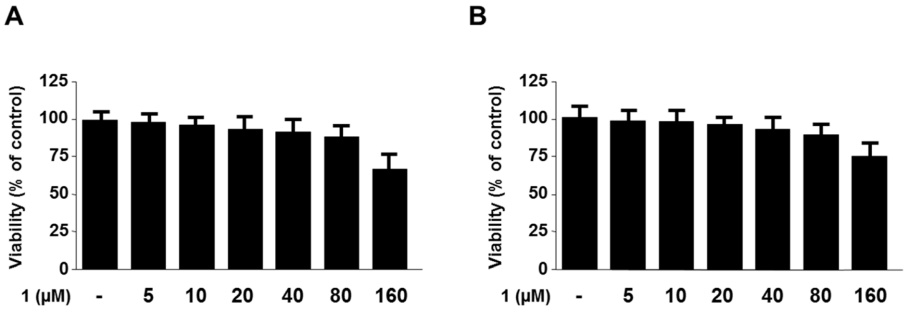

Fig. 2. Effects of **1** on cell viability. RAW264.7 (A) and BV2 cells (B) were incubated for 24 h with various concentrations of **1** (1 - 160 μM). Cell viability was determined by MTT assay. Each bar represents the mean ± S.D. of three independent experiments.

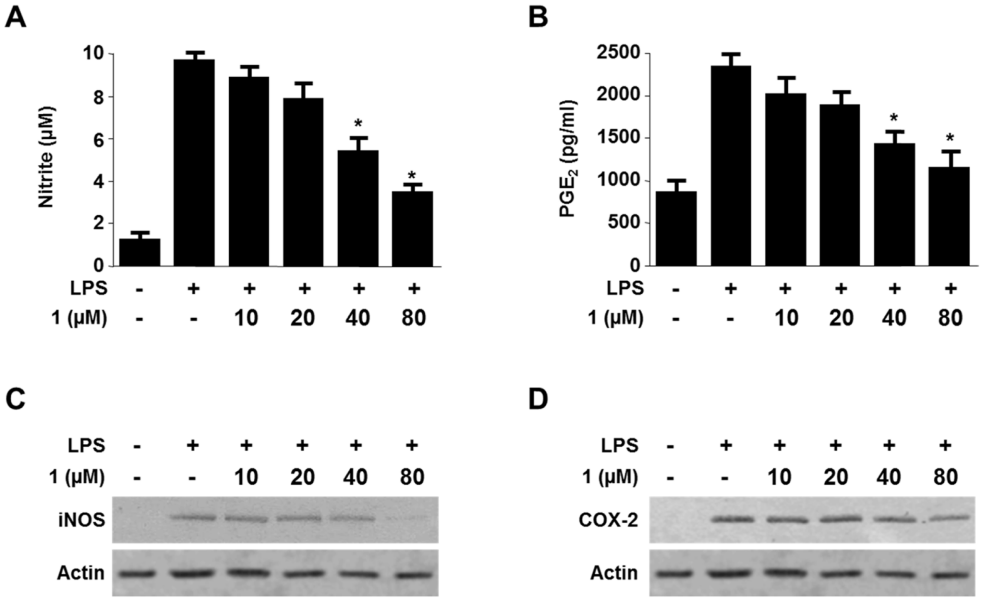

Fig. 3. Effects of **1** on the protein expression of nitrite (A), PGE_2 (B) iNOS (C) and COX-2 (D) in RAW 264.7 cells stimulated with LPS. The cells were pre-treated for 3 h with indicated concentrations of **1**, and then stimulated for 24 h with LPS (1 μg/mL). The concentrations of nitrite, PGE_2 and Western blot analysis were performed as described in the experimental section, and representative data of three independent experiments are shown. $^{*}p < 0.05$ compared with the LPS.

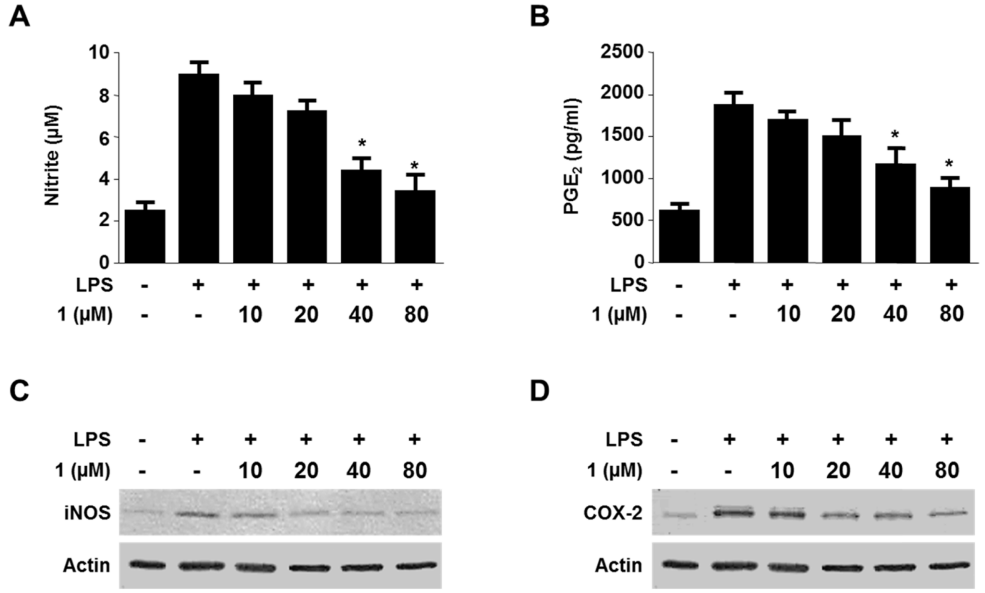

Fig. 4. Effects of **1** on the protein expression of nitrite (A), PGE_2 (B) iNOS (C) and COX-2 (D) in BV2 cells stimulated with LPS. The cells were pre-treated for 3 h with indicated concentrations of **1**, and then stimulated for 24 h with LPS (1 μg/mL). The concentrations of nitrite, PGE_2 and Western blot analysis were performed as described in the experimental section, and representative data of three independent experiments are shown. $^{*}p < 0.05$ compared with the LPS.

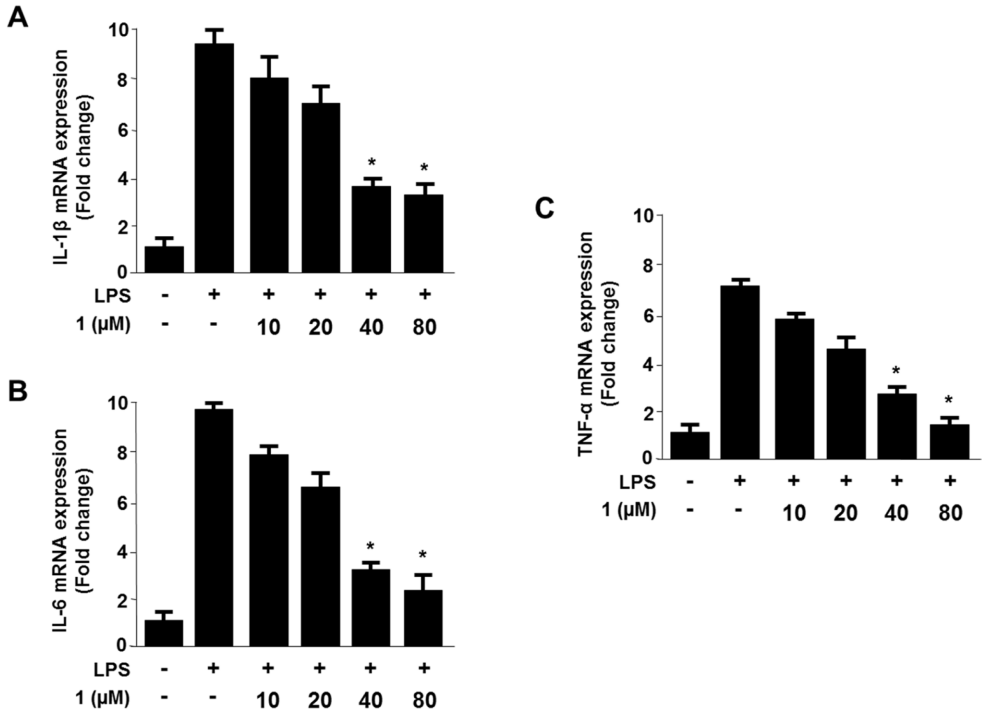

Fig. 5. Effects of **1** on IL-1β mRNA (A), IL-6 mRNA (B), and TNF-α mRNA (C) expression in RAW264.7 cells. Cells were incubated with the indicated concentrations of **1** for 3 h, and then treated for 6 h with LPS (1 μg/mL). RNA quantification for IL-1β, IL-6 and TNF-α expression were performed as described in the experimental section. Data shown represent the mean values of three independent experiments. $^{*}p < 0.05$ compared with the LPS.

To examine the anti-inflammatory effects of **1**, RAW264.7 and BV2 cells were pretreated with indicated concentration of **1** for 3 h before stimulated with LPS for 24 h. When the RAW264.7 and BV2 cells were treated

with LPS, the levels of pro-inflammatory mediators were significantly increased, however, pre-treatment of **1** markedly suppressed the concentrations of iNOS-derived NO with an IC_{50} value of 46.03 μM in RAW264.7 cells and 43.03 μM in BV2 cells (Figs. 3A and 4A). In addition, **1** was shown to inhibit the concentrations of COX-2-derived PGE_2 in these cells with an IC_{50} value of 30.37 μM and 34.20 μM, respectively (Figs. 3B and 4B). Furthermore, the protein expression of iNOS (Figs. 3C and 4C) and COX-2 (Figs. 3D and 4D) were also decreased in a dose dependent manner.

To further confirm the anti-inflammatory effect of the compound, the effects of **1** on the expression of mRNA levels of cytokines such as IL-1β, IL-6, and TNF-α in the LPS-stimulated cells were examined by qRT-PCR analysis. The cells were pre-incubated with the presence or absence of non-cytotoxic concentration range of **1** for 3 h before being stimulated with LPS (1 μg/mL) for 6 h. As a result, **1** decreased the mRNA expression of IL-1β, IL-6, and TNF-α in a dose-dependent manner in LPS-stimulated RAW264.7 cells (Fig. 5). In addition, compound **1** inhibited the mRNA expression of IL-1â and TNF-α, but did not affect IL-6 mRNA expression in LPS-stimulated BV2 cells (Fig. 6).

The transcription factor, NF-κB regulates various genes involved in the process of inflammatory and immune responses, cell adhesion, and survival.[18,19] NF-κB plays an important role in the transcriptional regulation of inflammatory mediators and cytokines.[20] In order to elucidate the mechanisms underlying the inhibition of iNOS and COX-2 protein expression by **1**, we examined the effects of **1** on the protein expression levels of phosphorylated IκB-α and degradation of IκB-α, an inhibitor associated with NF-κB in the cytoplasm. As shown in Figs. 7A and 8A, IκB-α was phosphorylated and degraded after treatment with LPS RAW264.7 and BV2 cells for 1 h, and these phosphorylation and degradation were markedly inhibited by pre-treatment of the cells with the indicated concentrations of **1** for 3 h. This result suggested that **1** inhibited the nuclear translocation of NF-κB (p65 and p50) by the stimulation of LPS through prevention of IκB-degradation. In a line with this, the protein levels of nuclear p65 and p50 proteins in RAW264.7 and BV2 cells were increased after treating the cells with LPS while the levels of p65 and p50 were declined in response to pre-treatment with the indicated concentrations of **1** for 3 h (Figs. 7B and 8B). Furthermore, compound **1** was shown to inhibit NF-κB–DNA binding

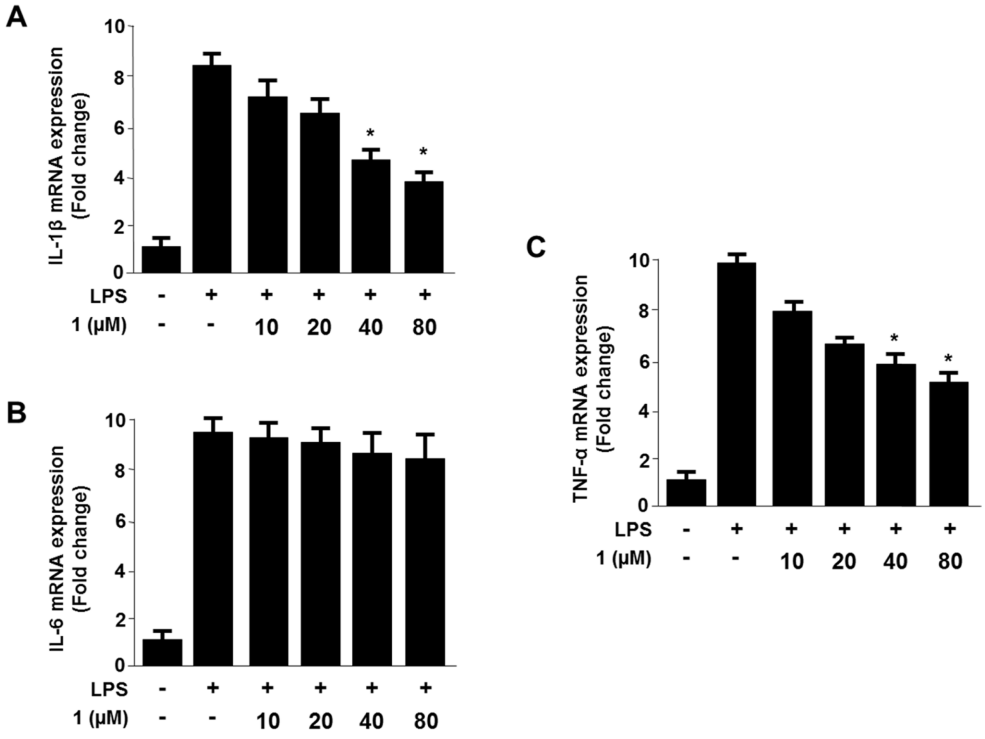

Fig. 6. Effects of **1** on IL-1β mRNA (A), IL-6 mRNA (B), and TNF-α mRNA (C) expression in BV2 cells. Cells were incubated with the indicated concentrations of **1** for 3 h, and then treated for 6 h with LPS (1 μg/mL). RNA quantification for IL-1β, IL-6 and TNF-α expression were performed, as described in the experimental section. Data shown represent the mean values of three independent experiments. $^{*}p < 0.05$ compared with the LPS.

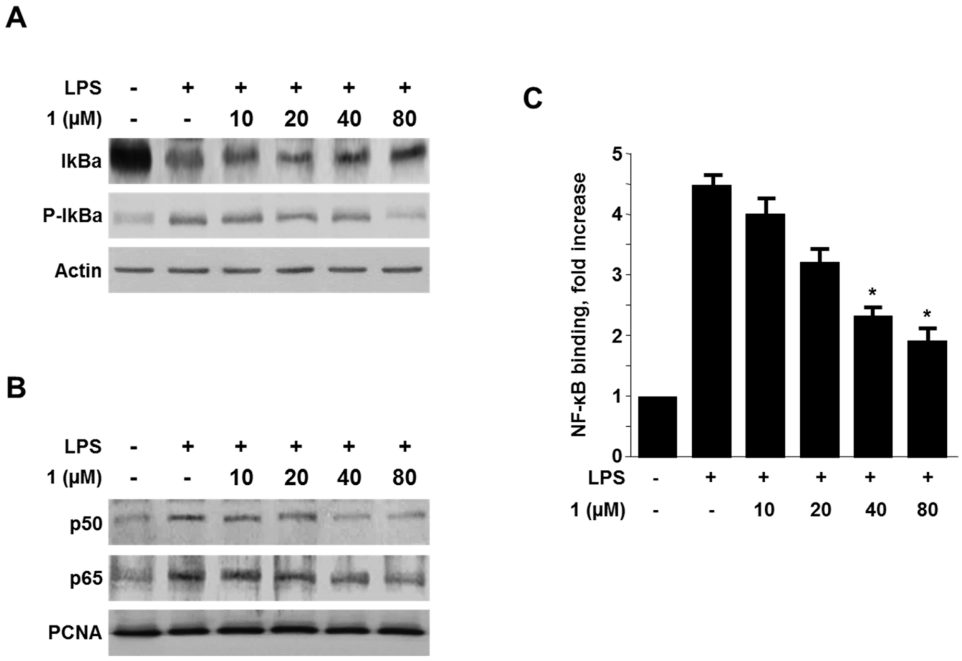

Fig. 7. Effects of **1** on the IκB-α phosphorylation and degradation (A), NF-κB activation (p65 and p50), and NF-κB DNA-binding activity (C). RAW264.7 cells were pre-treated with the indicated concentrations of 1 for 3 h, and then stimulated with LPS (1 μg/mL) for 1 h. The western blot analysis of IκBα and p-IκBα in the cytoplasm and NF-κB in the nucleus was performed as described in the experimental section. The representative blots of three independent experiments are shown. A commercially available NF-κB ELISA (Active Motif) was then used to test nuclear extracts and to determine the degree of NF-κB binding. The data represent the mean values of 3 experiments ± SD. $^{*}P < 0.05$ compared with the group treated with LPS.

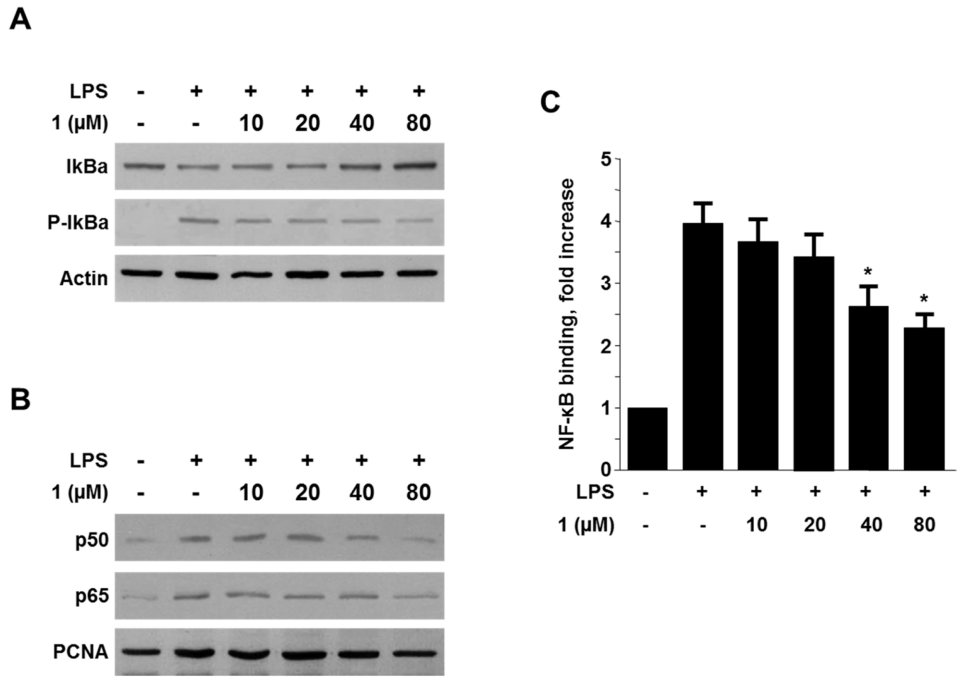

Fig. 8. Effects of **1** on the IκB-α phosphorylation and degradation (A), NF-κB activation (p65 and p50), and NF-κB DNA-binding activity (C). BV2 cells were pre-treated with the indicated concentrations of 1 for 3 h, and then stimulated with LPS (1 μg/mL) for 1 h. The western blot analysis of IκBα and p-IκBα in the cytoplasm and NF-κB in the nucleus was performed as described in the experimental section. The representative blots of three independent experiments are shown. A commercially available NF-κB ELISA (Active Motif) was then used to test nuclear extracts and to determine the degree of NF-κB binding. The data represent the mean values of 3 experiments ± SD. $^{*}P < 0.05$ compared with the group treated with LPS.

activity stimulated by LPS. As shown in Figs 7C and 8C, treatment with LPS alone increased the levels of NF-κB–DNA binding activity in the cells, while **1** inhibited the NF-κB-DNA binding activity in RAW264.7 and BV2 cells stimulated with LPS in a dose-dependent manner.

Conclusion

Marine natural products are a rich source of untapped bioactive metabolites. Marine microorganisms such as diverse bacteria, fungi, and algae are considered to be a great potential source of biodiversity. Noteworthy endeavors have been placed on the pharmacological investigation of marine-derived fungi.[21,22]

In macrophages and microglia, the activation of NF-κB signaling pathway plays a significant role in the regulation of immune and inflammatory responses. Thus, the inhibition of NF-κB pathway has been considered as an important therapeutic target for the treatment of inflammations in drug discovery, and several marine-derived metabolites have been evaluated for their potential to inhibit NF-κB pathway.[23,24] In our continuing investigation on the secondary metabolites from marine-derived fungi, viridicatol (**1**) has been isolated from cultivation of the marine-derived fungus *Penicillium* sp. SF-5295, it was shown that compound **1** inhibit PTP1B activity by binding to the active site within PTP1B.[15] In addition, cytotoxic effect of **1** against tumor cells has also been reported.[25] However, to the best of our knowledge, there have been no previous reports on the anti-inflammatory effects of **1**. In the present study, **1** shown to attenuate the production of pro-inflammatory mediators such as PGE_2 and NO, and also suppressed the protein expression of iNOS and COX-2 in LPS-stimulated RAW264.7 and BV2 cells. Next, in the further evaluation of the anti-inflammatory effects of **1**, pre-treatment with **1** in LPS-induced RAW264.7 and BV2 cells reduced the mRNA expression levels of IL-1β and IL-6, but TNF-α with the exception of IL-6 mRNA expression of LPS- induced BV2 cells. Moreover, our results revealed that **1** inhibited NF-κB signaling pathways by blocking the translocation of NF-κB heterodimer in nucleus and suppressing phosphorylation and degradation of IκB-α in cytoplasm.

Acknowledgments

We acknowledge financial support by grants from the Global R&D Center (GRDC, NRF-2010-00719) programs of the National Research Foundation of Korea (NRF) funded by the Ministry of Science, ICT and Future Planning of Korea (MSIFP).

References

(1) Ingersoll, M. A.; Platt, A. M.; Potteaux, S.; Randolph, G. J. *Trends Immunol*. **2011**, *32*, 470-477.
(2) Sosroseno, W.; Barid, I.; Herminajeng, E.; Susilowati, H. *Oral Microbiol. Immunol*. **2002**, *17*, 72-78.
(3) Block, M. L.; Zecca, L.; Hong, J. S. *Nat. Rev. Neurosci.* **2007**, *8*, 57-69.
(4) Jiang, F.; Ramanathan, A.; Miller, M. T.; Tang, G. Q.; Gale, M. Jr.; Patel, S. S.; Marcotrigiano, J. *Nature* **2011**, *479*, 423-427.
(5) Tsan, M. F.; Gao, B. *J. Endotoxin Res*. **2007**, *13*, 6-14.
(6) Yang, Y. Z.; Tang, Y. Z.; Liu, Y. H. *J. Ethnopharmacol*. **2013**, *148*, 271-276.
(7) Mizuno, T.; Kurotani, T.; Komatsu, Y.; Kawanokuchi, J.; Kato, H.; Mitsuma, N.; Suzumura, A. *Neuropharmacology* **2004**, *46*, 404-411.
(8) Ivashkiv, L. B. *Eur. J. Immunol*. **2011**, *41*, 2477-2481.
(9) Baldwin, A. S. Jr. *Annu. Rev. Immunol*. **1996**, *14*, 649-683.
(10) Mancino, A.; Lawrence, T. *Clin. Cancer Res*. **2010**, *16*, 784-789.
(11) Bremner, P.; Heinrich, M. *J. Pharm. Pharmacol*. **2002**, *54*, 453-472.
(12) Rateb, M. E.; Ebel, R. *Nat. Prod. Rep*. **2011**, *28*, 290-334.
(13) Bugni, T. S.; Ireland, C. M. *Nat. Prod. Rep*. **2004**, *21*, 143-163.
(14) Fremlin, L. J.; Piggott, A. M.; Lacey, E.; Capon, R. J. *J. Nat. Prod*. **2009**, *72*, 666-670.
(15) Sohn, J. H.; Lee, Y. R.; Lee, D. S.; Kim, Y. C.; Oh, H. *J. Microbiol. Biotechnol*. **2013**, *23*, 1206-1211.
(16) Berridge, M. V.; Tan, A. S. *Arch. Biochem. Biophys*. **1993**, *303*, 474-482.
(17) Titheradge, M. A. *Methods Mol. Biol*. **1998**, *100*, 83-91.
(18) Karin, M.; Ben-Neriah, Y. *Annu. Rev. Immunol*. **2000**, *18*, 621-663.
(19) Grilli, M.; Chiu, J. J.; Lenardo, M. J. *Int. Rev. Cytol*. **1993**, *143*, 1-62.
(20) Chen, F.; Sun, S. C.; Kuh, D. C.; Gaydos, L. J.; Demers, L. M. *Biochem. Biophys. Res. Commun*. **1995**, *214*, 985-992.
(21) Saleem, M.; Ali, M. S.; Hussain, S.; Jabbar, A.; Ashraf, M.; Lee, Y. S. *Nat. Prod. Rep.* **2007**, *24*, 1142-1152.
(22) Fenical, W.; Jensen, P. R. *Nat. Chem. Biol*. **2006**, *2*, 666-673.
(23) Lee, D. S.; Ko, W.; Quang, T. H.; Kim, K. S.; Sohn, J. H.; Jang, J. H.; Ahn, J. S.; Kim, Y. C.; Oh, H. *Mar. Drugs* **2013**, *11*, 4510-4526.
(24) Su, X.; Chen, Q.; Chen, W.; Chen, T.; Li, W.; Li, Y.; Dou, X.; Zhang, Y.; Shen, Y.; Wu, H.; Yu, C. *Int. Immunopharmacol*. **2014**, *19*, 88-93.
(25) Wei, M. Y.; Yang, R. Y.; Shao, C. L.; Wang, C. Y.; Deng, D. S.; She, Z. G.; Lin, Y. C. *Chem. Nat. Compd*. **2011**, *47*, 322-325.

Received June 29, 2015
Revised August 4, 2015
Accepted August 5, 2015